J Shoulder Elbow Surg (2019) 28, 2400–2408

ELSEVIER

Journal of Shoulder and Elbow Surgery

www.elsevier.com/locate/ymse

Validation of the registration accuracy of navigation-assisted arthroscopic débridement for elbow osteoarthritis

Atsuo Shigi, MD, Kunihiro Oka, MD, Hiroyuki Tanaka, MD, Shingo Abe, MD, Satoshi Miyamura, MD, Masaki Takao, MD, Tatsuo Mae, MD, Hideki Yoshikawa, MD, Tsuyoshi Murase, MD*

Department of Orthopaedic Surgery, Graduate School of Medicine, Osaka University, Suita, Osaka, Japan

Background: The identification and precise removal of bony impingement lesions during arthroscopic débridement arthroplasty for elbow osteoarthritis is technically difficult. Surgical navigation systems, combined with preoperative 3-dimensional (3D) assessment of bony impingements, can provide real-time tracking of the surgical instruments and impingement lesions. This study aims to determine the registration accuracy of the navigation system for the humerus and ulna during elbow arthroscopy.

Methods: We tested the registration procedure using resin bone models of 3 actual patients with elbow osteoarthritis. We digitized bone surface points using navigation pointers under arthroscopy. We initially performed paired-point registration, digitizing 6 preset anatomical landmarks, and then refined the initial alignment with surface matching registration, digitizing 30 points. The registration accuracy for each trial was evaluated as the mean target registration error in each reference marker. Three observers repeated the registration procedure 5 times each with the 3 specimens (total, 45 trials). The median of the registration accuracy was evaluated in total (45 trials) as the accuracy of the registration procedure. The differences in the registration accuracy among the 3 observers (median of 15 trials) were also examined.

Results: The total registration accuracies were 0.96 mm for the humerus and 0.85 mm for the ulna. No significant differences were found in the registration accuracy for the humerus and ulna among the 3 observers.

Conclusions: This arthroscopic-assisted registration procedure is sufficiently feasible and accurate for application of the navigation system to arthroscopic débridement arthroplasty in clinical settings.

Level of evidence: Basic Science Study; Computer Modeling

Keywords: Surgical navigation; registration accuracy; elbow arthroscopy; osteoarthritis; débridement arthroplasty; computer simulation

This study was approved by the Institutional Review Board of the Academic Clinical Research Center of Osaka University (Approval Number: 14179) and followed the tenets of the Declaration of Helsinki as revised in 2000.

*Reprint requests: Tsuyoshi Murase, MD, Department of Orthopaedic Surgery, Graduate School of Medicine, Osaka University, 2-2, Yamadaoka, Suita, Osaka 565-0871, Japan.

E-mail address: tmurase-osk@umin.ac.jp (T. Murase).

1058-2746/$ - see front matter
https://doi.org/10.1016/j.jse.2019.06.009

Symptomatic primary elbow osteoarthritis (OA) commonly occurs in middle-aged athletes and in individuals engaged in heavy manual labor.[1,32,33] Typical symptoms of elbow OA include pain, restricted range of motion (ROM), and joint catching and locking caused by loose bodies.[3,23] Radiography frequently reveals the presence of osteophytes and loose body formations on the olecranon and coronoid processes and the fossae, whereas the ulnohumeral joint is relatively well preserved.[7,36,39] Therefore, débridement arthroplasty, including synovectomy, loose body removal, capsular release, and impinging osteophytes removal, is recommended using an open[3,23,39] or arthroscopic procedure[1,10,15,17,34] for treating mild-to-moderate elbow OA. Arthroscopic débridement arthroplasty (ADA) is increasingly preferred because of the reduced intraoperative bleeding and postoperative pain, as well as early functional recovery.[24] However, these procedures are technically demanding because of the limited field of view and working space, as well as the close proximity to neurovascular structures. Moreover, the treating surgeons need to be careful not to miss any bony impingement lesions, because even small lesions can compromise the clinical outcome.

Preoperative radiologic assessments of the elbow joint using plain radiography and computed tomographic (CT) images provide useful information on the location and size of the osteophytes. However, these techniques are insufficient for precise identification of bony impingement lesions. On the contrary, technological advances in medical imaging have made it possible to analyze 3-dimensional (3D) kinematics of the elbow joint using 3D computer bone models reconstructed from CT data.[11,12,21] This technique provides preoperative visual 3D images for assessments of bony impingement lesions that need to be removed to achieve optimal elbow ROM.[22,40] However, the bony impingement lesions cannot be easily removed according to the preoperative 3D assessment plan because of difficulty in acquiring an accurate spatial sense under elbow arthroscopy, considering the shape of the bone surface changes while removing the osteophytes. Accordingly, we focused on ADA for elbow OA using a surgical navigation system in combination with a preoperative 3D assessment. The aim of our study was to determine the registration accuracy of the navigation system for elbow arthroscopic procedures.

Materials and methods

This is a validation study of the registration accuracy of the navigation system for an elbow arthroscopic procedure using an arthroscopy simulator. Several published registration accuracy validation studies in orthopedic surgery have used plastic bone models or cadavers; however, few studies have considered the restricted operation of a navigation pointer under arthroscopic conditions.[4,8,20,37] In addition, the shape of the intracapsular bone surface of patients with OA differs from that of normal individuals, which may affect the registration accuracy. 3D-printed bone models of actual patients based on CT data have been used for surgical simulations and validation studies, because these models display patient-specific anatomical pathologies.[16,18] Therefore, we designed a validation study using an arthroscopy simulator with 3D-printed resin bone models of actual patients with elbow OA.

Specimens

We randomly extracted CT data of 3 men with primary elbow OA from our institution's database. All patients underwent ADA based on the preoperative 3D assessments of bony impingement lesions at our institute.[22] We acquired CT images of the whole humerus, radius, and ulna using a helical CT scanner (LightSpeed Ultra 16; General Electric, Waukesha, WI, USA) with a low-dose radiation protocol: 120-kV tube voltage, 30-mA current, 1.25-mm-thick slices, and 0.48-mm pixel size.[26] We sent CT data to a workstation in Digital Imaging and Communications in Medicine (DICOM) format. The 3D computer bone models of the humerus, ulna, and radius were reconstructed in Standard Triangulation Language format from CT data with a dedicated threshold-based segmentation software (BoneViewer; Orthree, Osaka, Japan) using a 200–Hounsfield units threshold.[27,28] We designated the distal humerus and proximal ulna as the target regions for surgical navigation because osteophytes are usually removed from the coronoid and olecranon fossae and from the tips of the coronoid and olecranon processes. We defined 4 ground truth reference points (RP_{GT}s) on the surface of the distal humerus (1, immediately proximal to the olecranon fossa; 2, medial epicondyle; 3, lateral epicondyle; and 4, immediately proximal to the coronoid fossa) and proximal ulna (1, tip of the olecranon; 2, medial aspect of the olecranon; 3, lateral aspect of the olecranon; and 4, coronoid process) using planning software (BoneSimulator; Orthree)[27,28] to evaluate the registration accuracy in the periarticular region of the elbow (Fig. 1). We also created hemispherical markers (3.0 mm in diameter) as reference points on the bone models. A dimple at the center of each marker suitably accommodated the tip of a navigation pointer to digitize the reference points precisely (Fig. 2). We created the resin bone models, including reference markers, using acrylic compounds (VeroWhitePlus-RGD835; Stratasys, Eden Prairie, MN, USA) and a 3D printer (Objet prime 30; Stratasys) with a 0.1-mm 3D shaping accuracy. We linked the resin bone models with elastic bundles that mimicked collateral and annular ligaments to allow passive movement of the elbow during arthroscopy. We determined the size of the intracapsular area available for digitalization of the registration procedure under arthroscopy, avoiding the area that would be covered with articular cartilage because the thickness of the cartilage might cause matching errors between the surface data of an actual patient and the computer bone model constructed from CT data. We drew the boundary of the intracapsular areas on the bone models with a permanent marker according to the model in a previous anatomical study (Fig. 3, *A* and *B*).[31]

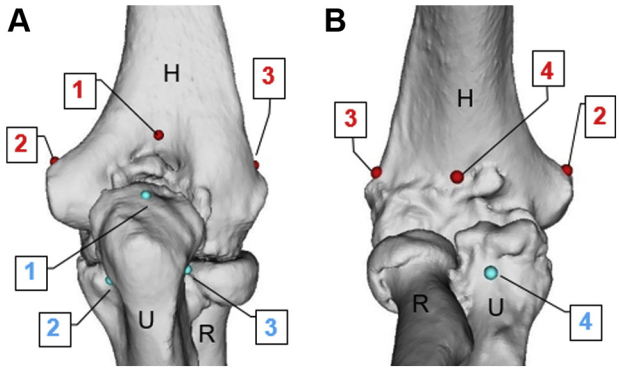

Figure 1 Computer bone models created from computed tomography data. Posterior (**A**) and anterior (**B**) views. Four ground truth reference points were defined on the distal humerus (*red* 1, immediately proximal to the olecranon fossa; 2, medial epicondyle; 3, lateral epicondyle; and 4, immediately proximal to the coronoid fossa) and the proximal ulna (*blue* 1, tip of the olecranon; 2, medial aspect of the olecranon; 3, lateral aspect of the olecranon; and 4, the coronoid process).

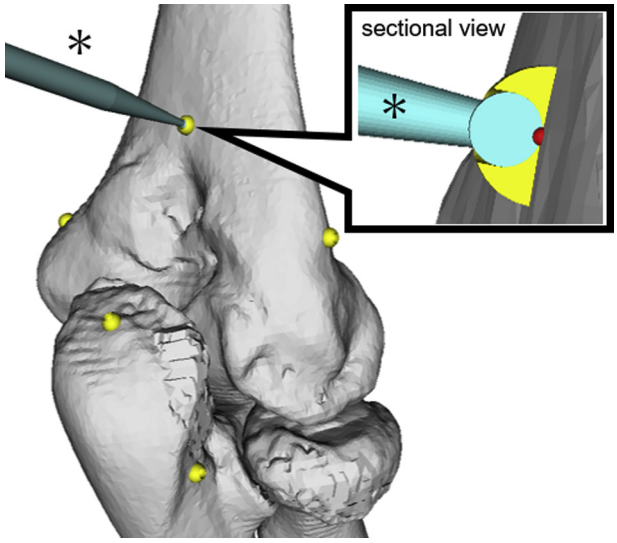

Figure 2 Reference markers on the bone models. The hemispherical reference markers (*yellow*) had dimples at the center that suitably accommodated the tip of the navigation pointer (*) to correctly digitize the reference points (*red*).

Arthroscopy simulator

The elbow arthroscopy simulator for this study was based on those in studies of arthroscopy simulator surgical training for novices in shoulder and knee surgery.[2,29,30] The simulator consisted of the resin bone models, enclosed in rubber skin and spongy subcutaneous tissue (#1411 arthroscopic elbow; Sawbones, Vashon, WA, USA) (Fig. 3, *C*), and clamps. To simulate the elbow arthroscopy in the prone position, with the shoulder at 90° abduction and the forearm dropping, we fixed the bone models at the proximal humerus on a table using a clamp (Fig. 4, *A*). We set an arthroscopy tower (Smith & Nephew, London, UK), including a monitor, camera system, and light source, on the proximal side of the humerus. We used a 2.7-mm × 30° scope (Smith & Nephew) and a 5-portal technique for the elbow arthroscopies, palpating the anterior intracapsular areas through the proximal anteromedial and anterolateral portals. Direct posterior, posterolateral, and soft spot portals were used to palpate the posterior intracapsular area (Fig. 4, *B-E*).

Preparing the navigation system

We used an optical computer navigation system with a 0.070 ± 0.032-mm optical localizer accuracy[9] (Stryker Navigation System II Cart; Stryker, Kalamazoo, MI, USA) to perform the navigation procedure. We imported the original CT data into the 3D navigation and planning software (Orthomap, Stryker) in the DICOM format, and reconstructed the 3D bone model in the navigation system with the same Hounsfield unit threshold using BoneViewer software. The placement of 2 dynamic reference trackers was decided manually. We placed the humeral tracker on the dorsolateral safe zone of the distal humerus to avoid radial nerve injury. This area is located proximally along the lateral humeral shaft, from the lateral epicondyle to the level of the transepicondylar distance, where the radial nerve crosses the humerus in the midlateral plane.[14] Subsequently, we placed the ulnar tracker on the dorsal aspect of the proximal ulna, avoiding the extensor carpi ulnaris and flexor carpi ulnaris muscles. We fixed 2 dynamic reference trackers to the humerus and the ulna using two 3-mm-diameter half pins and clamps of an external fixator system (Hoffman II system; Stryker) through small incisions. We decided the positions of the dynamic reference trackers so as to avoid interrupting the arthroscopy and navigation pointer operations (Fig. 4, *A*).

Before evaluating the registration accuracy, we conducted a preliminary validation of the sampling precision of the digitizing reference markers in the navigation system. One researcher (A.S.) manually and repeatedly digitized the same reference marker 20 times with the navigation pointer perpendicular to the bone surface and recorded these coordinates. We validated the sampling precision based on the standard deviation of the distance between the reference point and the origin of the coordinate system of the navigation system.

Registration procedure

Three researchers (A.S., S.M., and S.A.) used 3 specimens to perform the registration procedures. A.S. built the registration protocol using planning software (Orthomap, Stryker), and S.M. and S.A. carefully reviewed the registration protocol. Paired-point registration (PPR) was initially performed, and the initial alignment was then refined with surface matching registration (SMR) based on the iterative closest point algorithm.[5] We performed point acquisition for PPR and SMR using the navigation pointer. PPR was performed by digitizing 6 preset anatomical landmarks for the humerus (radial fossa, coronoid fossa, 2 points on the olecranon fossa under arthroscopy, and tips of the medial and lateral epicondyles through small incisions) (Fig. 5, *A*) and for the ulna (the lateral and medial tips of both the coronoid process and olecranon under arthroscopy, the dorsal aspect of the olecranon, and the styloid process through a small incision) (Fig. 5, *B*). We considered a mean deviation of fiducial

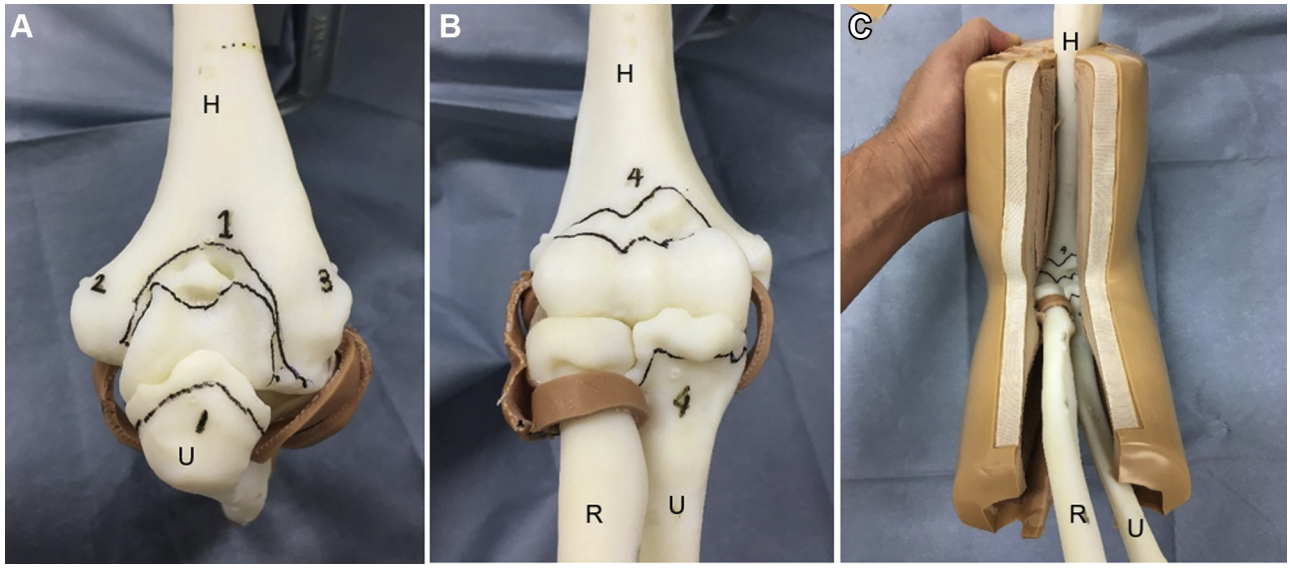

Figure 3 Resin bone models created by the 3D printer. Posterior (**A**) and anterior (**B**) views. The black line on the resin bone models indicates the boundary of the intracapsular area available for digitizing. (**C**) A resin bone model was enclosed in a rubber skin and subcutaneous sponge (#1411 arthroscopic elbow; Sawbones). *H*, humerus; *U*, ulna; *R*, radius.

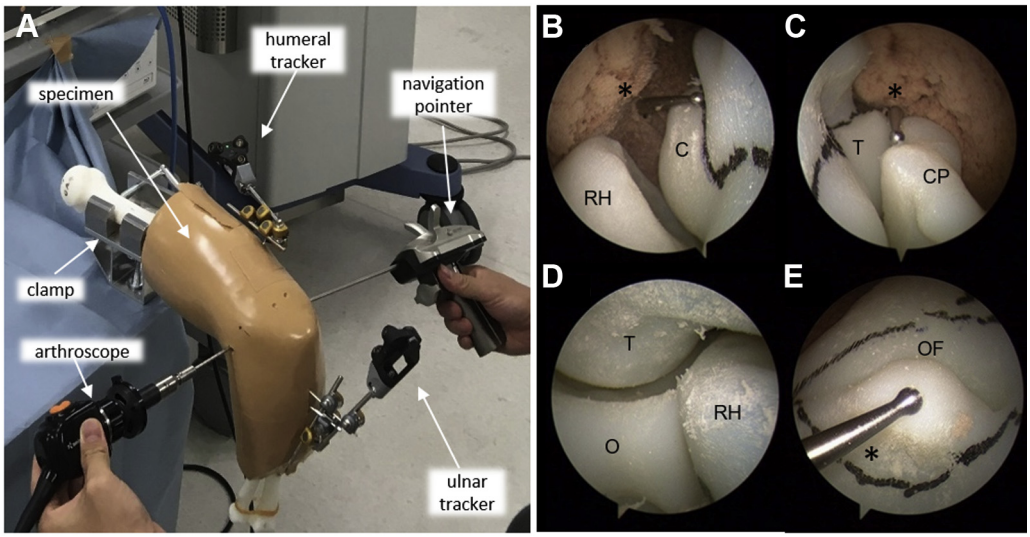

Figure 4 Arthroscopy simulator Overview (**A**). Arthroscopic view from the proximal anteromedial portal (**B**), anterolateral portal (**C**), soft spot portal (**D**), and posterolateral portal with the arthroscopy simulator (**E**). *, navigation pointer; *T*, trochlea; *CP*, coronoid process; *RH*, radial head; *C*, capitellum; *O*, olecranon; *OF*, olecranon fossa.

registration error of less than 2.0 mm displayed by the navigation system after PPR as acceptable. If the mean deviation was more than 2.0 mm, we redigitized the landmark. Consecutive SMR was performed by digitizing 30 points on the bone surface, according to a published result.[35] As for the digitizing area, distant surfaces on the distal humerus have been reported to assist in constraining the surfaces together during SMR and to improve the registration accuracy.[20] Therefore, we digitized both intracapsular and extracapsular surfaces on the distal humerus and proximal ulna to maximize the distance between one surface and the other one. For the humerus, a researcher digitized 7 intracapsular points each on the anterior and posterior intracapsular surfaces, 4 extracapsular points on the medial epicondyle, 4 points on the lateral epicondyle, and 8 points on the dorsolateral surfaces of the humeral shaft around the insertion of the fixation pin for the humeral tracker (Fig. 6, *A-C*). For the ulna, the researcher digitized 8 intracapsular points on the anterior intracapsular surface, 10 intracapsular points on the posterior intracapsular surface, 4 extracapsular points on the tip of the olecranon, and 8 extracapsular points on the dorsal surfaces of the ulnar diaphysis around the insertion of the fixation pin for the ulnar tracker (Fig. 6, *D-F*). To avoid a learning curve bias, all 3 researchers practiced the registration procedure 3 times before the registration trials.

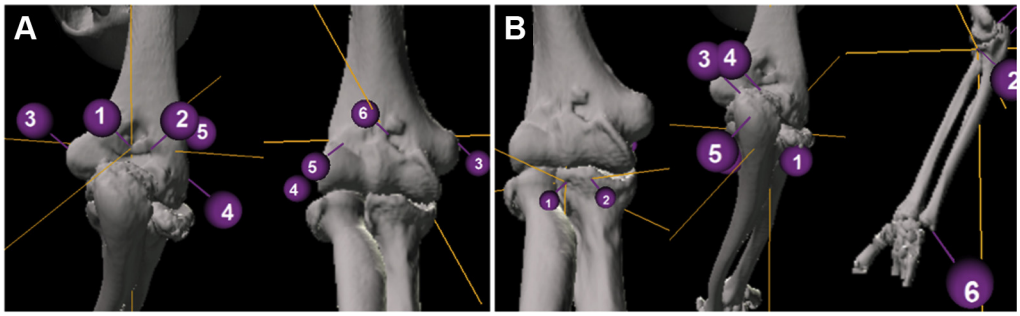

Figure 5 Six anatomical landmarks for paired-point registration. (**A**) Anatomical landmarks for the humerus (1 and 2, middle and lateral points on the olecranon fossa; 3, tip of the medial epicondyle; 4, tip of the lateral epicondyle; 5, radial fossa; and 6, coronoid fossa); (**B**) for the ulna (1 and 2, lateral and medial tips of the coronoid process; 3 and 4, lateral and medial tips of the olecranon; 5, dorsal aspect of the olecranon; 6, styloid process).

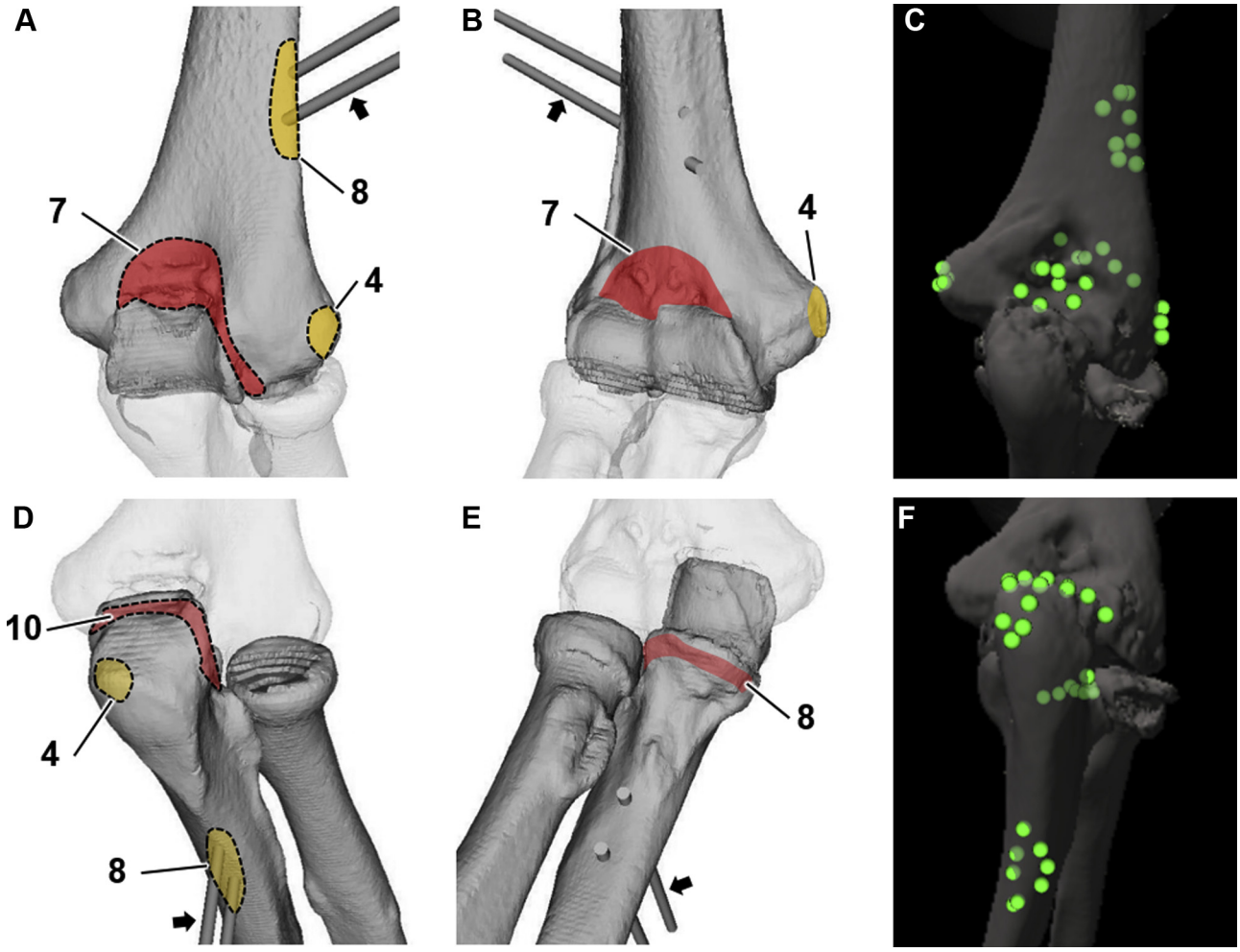

Figure 6 Digitization area for surface matching registration of the humerus (**A**-**C**) and ulna (**D**-**F**). Red area, intracapsular area; *yellow* area, extracapsular area; ➡ half pin for tracker fixation; and ➡ pointing to the colored area, number of digitizing points. The *green dots* in **C** correspond to the numbers shown in **A** and **B** and those in **F** to the numbers in **D** and **E**. The actual point set for surface matching registration displayed by Orthomap (*Stryker*) is shown in **C** and **F**.

Table I Registration accuracies by each researcher and in total

	n	Mean TRE, mm		*P* values*		
		Median	Interquartile range	RSR 1 vs. 2	RSR 2 vs. 3	RSR 1 vs. 3
Humerus						
RSR 1	15	0.99	0.80-1.31	.93	.87	.50
RSR 2	15	0.91	0.76-1.28			
RSR 3	15	0.84	0.69-1.08			
Total	45	0.96	0.71-1.20			
Ulna						
RSR 1	15	0.92	0.65-1.27	>.99	.99	.91
RSR 2	15	0.82	0.71-1.11			
RSR 3	15	0.85	0.72-0.97			
Total	45	0.85	0.71-1.18			

TRE, mean target registration error; *RSR*, researcher.
* Multiple comparisons among researchers using the Steel-Dwass test.

Evaluation of the registration accuracy

After the registration procedure, we removed the soft tissue from the resin bone models to palpate the reference markers using the navigation pointer. We digitized the 4 reference markers each on the humerus and ulna according to the coordinates of the navigation system. These coordinates were transformed into the coordinate system of the BoneSimulator software as the registered reference points (RP_{REG}'s). We calculated the target registration error (TRE) as the distance between corresponding RP_{GT} and RP_{REG}. We calculated the mean TRE of the 4 reference points as the registration accuracy of each registration procedure. Three researchers repeated the registration procedure and mean TRE evaluation 5 times with 3 specimens each (for a total of 45 trials). We evaluated the total registration accuracy using the median of the mean TRE of the 45 trials. The differences in the registration accuracy among the 3 researchers were also evaluated using the median of 15 trials.

Statistical analysis

All statistical analyses were performed using the JMP Pro 12.2.0 software (SAS, Cary, NC, USA). Shapiro-Wilk test was used to determine normality of the data distribution. Data are presented as medians and interquartile ranges (IQRs). Differences in the registration accuracy among the 3 researchers were evaluated using the Steel-Dwass test. We considered P values $<.05$ as statistically significant.

Results

The sampling precision of the reference points using the navigation system was 0.06 mm, which was similar to the optical localizer error of the navigation system.[9] Table I shows the registration accuracy of our registration procedure. The total registration accuracy was 0.96 mm (IQR, 0.71-1.20 mm) for the humerus and 0.85 mm (IQR, 0.71-1.18 mm) for the ulna. The IQRs showed that our registration procedure achieved <1.20-mm registration accuracy for the humerus and 1.18-mm registration accuracy for the ulna, with a 75% probability. Of the 45 trials of the humerus, 2 (4.4%) resulted in a TRE of >2 mm. We found no significant differences in the registration accuracies among the 3 researchers (Fig. 7).

Discussion

Application of a surgical navigation system, combined with preoperative 3D assessment of bony impingement lesions, could provide real-time tracking of both the surgical instruments and bony impingement lesions.[22,40] Navigation systems for arthroscopic surgery have been used for the knee, hip, ankle, and shoulder[6,13,25,38]; however, to our knowledge, no validations for elbow arthroscopy have been published to date.

Different types of surgical navigation systems, including CT-based, fluoroscopy-based, and image-free systems, are available for orthopedic surgery.[19] One advantage of CT-based navigation systems is that they can be combined with preoperative 3D assessments of bony impingement lesions. For this study, we adopted an imageless registration technique to digitize the bone surface data because imageless registration does not require a 3D C-arm CT and additional radiation exposure. To determine the registration set point, we referred to a validation study that used imageless registration with a small portion of the articular surface and the shaft of the distal humerus during an open procedure of the elbow.[20] This study described the humeral shaft surface as a significant landmark in the registration process.[20] We determined the point sets in a manner that allowed for digitization of the intracapsular points under arthroscopy and the extracapsular points on the shafts of the humerus and ulna through small incisions for tracker placement. Thus, our registration protocol is feasible for use during actual elbow arthroscopies.

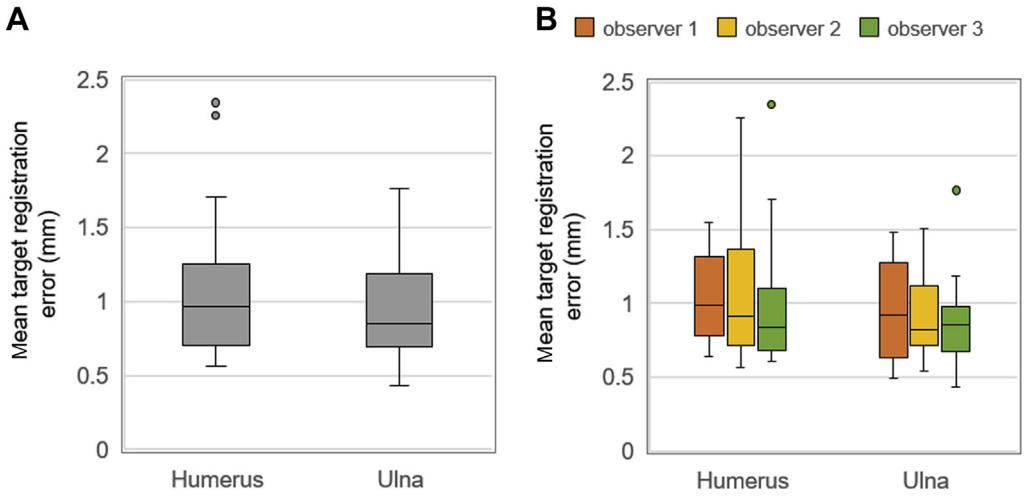

Figure 7 Box plot of the mean target registration error (mm). Mean target registration error in total (**A**) and by each researcher (**B**). Open circles represent statistical outliers.

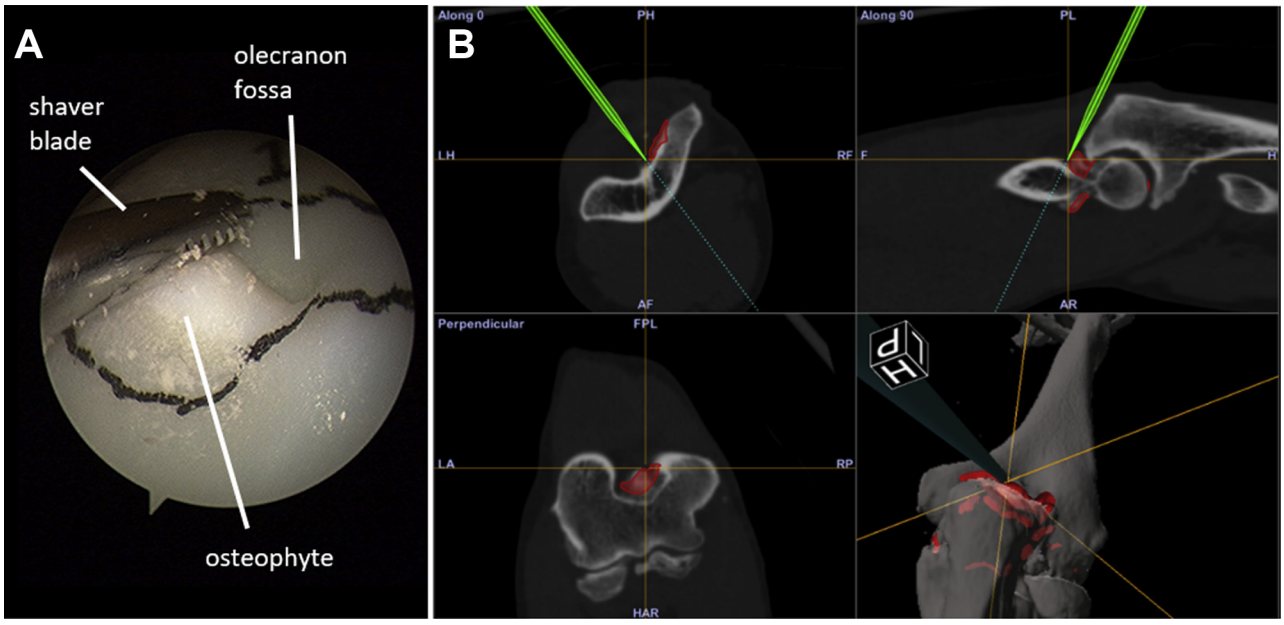

Figure 8 Navigation-assisted arthroscopy combined with preoperative 3D assessment of bony impingement lesions. (**A**) Arthroscopic view from the posterolateral portal showing the tip of the calibrated shaver blade. (**B**) The navigation system displays real-time tracking of impingement lesion (*red*) and the tip of the calibrated shaver blade (*green*) during arthroscopic débridement arthroplasty.

Bony impingement lesions and surgical instruments, such as chisels, shaver blades, and abrader burrs, could be tracked in real-time with reasonable accuracy using the navigation system (Fig. 8). However, the TRE was >2 mm with 4.4% probability in the humerus. This may have been caused by error of PPR for the humerus. Unlike the 6 anatomical landmarks on the ulna that included the ulnar styloid process distant from the other landmarks, the 6 anatomical landmarks on the humerus were determined only on the distal humerus for PPR because it was difficult to identify and digitize the extracapsular anatomical landmarks on the middle and proximal part of the humerus. Thus, the 6 anatomical landmarks of the distal humerus for PPR were close to each other, which may have caused a large registration error on the proximal humerus after PPR. The iterative closest point algorithm for SMR requires a good initial alignment after PPR[20]; therefore, the registration error of the humerus may occasionally be large. Accordingly, it would be necessary to visually confirm the arthroscopic findings and navigation screen for the humerus. If the discrepancy between them is visually observed, the registration procedure should be repeated to refine the registration accuracy.

We are aware of the limitations in our study. First, we used an arthroscopy simulator that consisted of a resin bone model of actual patients with elbow OA and mimicked soft tissues to approximate the conditions in an actual surgery, but our specimen did not include cartilage, capsule, or synovium around the intracapsular area, which may have affected the registration accuracy. Second, in clinical settings, differences in shape between the actual bone and the 3D computer bone model reconstructed from 1.25-mm-slice CT data (our protocol of CT) may cause a registration error. Unlike under clinical settings, we used resin bone models created from CT data by a 3D printer. The surface difference between the 3D computer bone models and the resin bone model entirely depended on the accuracy of the 3D printer (0.1 mm). Therefore, we may have underestimated the error in this study compared with that in an actual clinical setting. Finally, our study validated the registration accuracy of the navigation system for elbow OA but not the accuracy of removal of bony impingement lesions. Therefore, verifying the accuracy of bony débridement for clinical application in the future is warranted.

Overall, this preliminary validation study using an arthroscopy simulator provided evidence suggesting that arthroscopic-assisted registration is feasible and reasonably accurate for ADA. Although this finding needs further clinical confirmation and validation before implementation during actual surgeries, a navigation system can facilitate accurate identification and removal of bony impingement lesions.

Conclusions

The arthroscopic-assisted registration procedure is sufficiently feasible and accurate for application of the navigation system to arthroscopic débridement arthroplasty in clinical settings.

Disclaimer

This work was supported by JSPS (Japan Society for the Promotion of Science, Japan) KAKENHI Grant Number JP 15K10442 and JP 15H04957.

Kunihiro Oka received funding in support of this research from the Japan Society for the Promotion of Science.

Tsuyoshi Murase received funding in support of this research from the Japan Society for the Promotion of Science.

The other authors, their immediate families, and any research foundations with which they are affiliated have not received any financial payments or other benefits from any commercial entity related to the subject of this article.

References

1. Adams JE, Wolff LH 3rd, Merten SM, Steinmann SP. Osteoarthritis of the elbow: results of arthroscopic osteophyte resection and capsulectomy. J Shoulder Elbow Surg 2008;17:126-31. https://doi.org/10.1016/j.jse.2007.04.005
2. Angelo RL, Pedowitz RA, Ryu RK, Gallagher AG. The Bankart performance metrics combined with a shoulder model simulator create a precise and accurate training tool for measuring surgeon skill. Arthroscopy 2015;31:1639-54. https://doi.org/10.1016/j.arthro.2015.04.092
3. Antuna SA, Morrey BF, Adams RA, O'Driscoll SW. Ulnohumeral arthroplasty for primary degenerative arthritis of the elbow: long-term outcome and complications. J Bone Joint Surg Am 2002;84:2168-73.
4. Audenaert E, Smet B, Pattyn C, Khanduja V. Imageless versus image-based registration in navigated arthroscopy of the hip: a cadaver-based assessment. J Bone Joint Surg Br 2012;94:624-9. https://doi.org/10.1302/0301-620x.94b5.28627
5. Besl PJ, McKay ND. A method for registration of 3-D shapes. IEEE Trans Pattern Anal Mach Intell 1992;14:239-56.
6. Brunner A, Horisberger M, Herzog RF. Evaluation of a computed tomography-based navigation system prototype for hip arthroscopy in the treatment of femoroacetabular cam impingement. Arthroscopy 2009;25:382-91. https://doi.org/10.1016/j.arthro.2008.11.012
7. Dalal S, Bull M, Stanley D. Radiographic changes at the elbow in primary osteoarthritis: a comparison with normal aging of the elbow joint. J Shoulder Elbow Surg 2007;16:358-61. https://doi.org/10.1016/j.jse.2006.08.005
8. Docquier PL, Paul L, Cartiaux O, Banse X. Registration accuracy in computer-assisted pelvic surgery. Comput Aided Surg 2009;14:37-44. https://doi.org/10.3109/10929080903024361
9. Elfring R, de la Fuente M, Radermacher K. Assessment of optical localizer accuracy for computer aided surgery systems. Comput Aided Surg 2010;15:1-12. https://doi.org/10.3109/10929081003647239
10. Galle SE, Beck JD, Burchette RJ, Harness NG. Outcomes of elbow arthroscopic osteocapsular arthroplasty. J Hand Surg 2016;41:184-91. https://doi.org/10.1016/j.jhsa.2015.11.018
11. Goto A, Moritomo H, Murase T, Oka K, Sugamoto K, Arimura T, et al. In vivo elbow biomechanical analysis during flexion: three-dimensional motion analysis using magnetic resonance imaging. J Shoulder Elbow Surg 2004;13:441-7. https://doi.org/10.1016/s1058274604000394
12. Goto A, Murase T, Moritomo H, Oka K, Sugamoto K, Yoshikawa H. Three-dimensional in vivo kinematics during elbow flexion in patients with lateral humeral condyle nonunion by an image-matching technique. J Shoulder Elbow Surg 2014;23:318-26. https://doi.org/10.1016/j.jse.2013.11.010
13. Hiraoka H, Kuribayashi S, Fukuda A, Fukui N, Nakamura K. Endoscopic anterior cruciate ligament reconstruction using a computer-assisted fluoroscopic navigation system. J Orthop Sci 2006;11:159-66. https://doi.org/10.1007/s00776-005-0988-3
14. Kamineni S, Ankem H, Patten DK. Anatomic relationship of the radial nerve to the elbow joint: clinical implications of safe pin placement. Clin Anat 2009;22:684-8. https://doi.org/10.1002/ca.20831
15. Kelly EW, Bryce R, Coghlan J, Bell S. Arthroscopic débridement without radial head excision of the osteoarthritic elbow. Arthroscopy 2007;23:151-6. https://doi.org/10.1016/j.arthro.2006.10.008
16. Kitada M, Sakai T, Murase T, Hanada T, Nakamura N, Sugano N. Validation of the femoral component placement during hip resurfacing: a comparison between the conventional jig, patient-specific template, and CT-based navigation. Int J Med Robot 2013;9:223-9. https://doi.org/10.1002/rcs.1490
17. Krishnan SG, Harkins DC, Pennington SD, Harrison DK, Burkhead WZ. Arthroscopic ulnohumeral arthroplasty for degenerative arthritis of the elbow in patients under fifty years of age. J Shoulder Elbow Surg 2007;16:443-8. https://doi.org/10.1016/j.jse.2006.09.001

18. Manganaro MS, Morag Y, Weadock WJ, Yablon CM, Gaetke-Udager K, Stein EB. Creating three-dimensional printed models of acetabular fractures for use as educational tools. Radiographics 2017; 37:871-80. https://doi.org/10.1148/rg.2017160129
19. Mavrogenis AF, Savvidou OD, Mimidis G, Papanastasiou J, Koulalis D, Demertzis N, et al. Computer-assisted navigation in orthopedic surgery. Orthopedics 2013;36:631-42. https://doi.org/10.3928/01477447-20130724-10
20. McDonald CP, Beaton BJ, King GJ, Peters TM, Johnson JA. The effect of anatomic landmark selection of the distal humerus on registration accuracy in computer-assisted elbow surgery. J Shoulder Elbow Surg 2008;17:833-43. https://doi.org/10.1016/j.jse.2008.02.007
21. Miyake J, Shimada K, Moritomo H, Kataoka T, Murase T, Sugamoto K. Kinematic changes in elbow osteoarthritis: in vivo and 3-dimensional analysis using computed tomographic data. J Hand Surg 2013;38:957-64. https://doi.org/10.1016/j.jhsa.2013.02.006
22. Miyake J, Shimada K, Oka K, Tanaka H, Sugamoto K, Yoshikawa H, et al. Arthroscopic débridement in the treatment of patients with osteoarthritis of the elbow, based on computer simulation. Bone Joint J 2014;96-b:237-41. https://doi.org/10.1302/0301-620x.96b2.30714
23. Morrey BF. Primary degenerative arthritis of the elbow. Treatment by ulnohumeral arthroplasty. J Bone Joint Surg Br 1992;74:409-13.
24. O'Driscoll SW. Arthroscopic treatment for osteoarthritis of the elbow. Orthop Clin North Am 1995;26:691-706.
25. O'Loughlin PF, Kendoff D, Pearle AD, Kennedy JG. Arthroscopic-assisted fluoroscopic navigation for retrograde drilling of a talar osteochondral lesion. Foot Ankle Int 2009;30:70-3. https://doi.org/10.3113/fai.2009.0070
26. Oka K, Murase T, Moritomo H, Goto A, Sugamoto K, Yoshikawa H. Accuracy analysis of three-dimensional bone surface models of the forearm constructed from multidetector computed tomography data. Int J Med Robot 2009;5:452-7. https://doi.org/10.1002/rcs.277
27. Omori S, Murase T, Kataoka T, Kawanishi Y, Oura K, Miyake J, et al. Three-dimensional corrective osteotomy using a patient-specific osteotomy guide and bone plate based on a computer simulation system: accuracy analysis in a cadaver study. Int J Med Robot 2014; 10:196-202. https://doi.org/10.1002/rcs.1530
28. Oura K, Oka K, Kawanishi Y, Sugamoto K, Yoshikawa H, Murase T. Volar morphology of the distal radius in axial planes: a quantitative analysis. J Orthop Res 2015;33:496-503. https://doi.org/10.1002/jor.22780
29. Peres LR, Junior WMA, Coelho G, Lyra M. A new simulator model for knee arthroscopy procedures. Knee Surg Sports Traumatol Arthrosc 2017;25:3076-83. https://doi.org/10.1007/s00167-016-4099-9
30. Rebolledo BJ, Hammann-Scala J, Leali A, Ranawat AS. Arthroscopy skills development with a surgical simulator: a comparative study in orthopaedic surgery residents. Am J Sports Med 2015;43:1526-9. https://doi.org/10.1177/0363546515574064
31. Reichel LM, Morales OA. Gross anatomy of the elbow capsule: a cadaveric study. J Hand Surg 2013;38:110-6. https://doi.org/10.1016/j.jhsa.2012.09.031
32. Rettig LA, Hastings H 2nd, Feinberg JR. Primary osteoarthritis of the elbow: lack of radiographic evidence for morphologic predisposition, results of operative débridement at intermediate follow-up, and basis for a new radiographic classification system. J Shoulder Elbow Surg 2008;17:97-105. https://doi.org/10.1016/j.jse.2007.03.014
33. Sarris I, Riano FA, Goebel F, Goitz RJ, Sotereanos DG. Ulnohumeral arthroplasty: results in primary degenerative arthritis of the elbow. Clin Orthop Relat Res 2004:190-3.
34. Steinmann SP, King GJ, Savoie FH 3rd, American Academy of Orthopaedic Surgeons. Arthroscopic treatment of the arthritic elbow. J Bone Joint Surg Am 2005;87:2114-21.
35. Sugano N, Sasama T, Sato Y, Nakajima Y, Nishii T, Yonenobu K, et al. Accuracy evaluation of surface-based registration methods in a computer navigation system for hip surgery performed through a posterolateral approach. Comput Aided Surg 2001;6:195-203.
36. Suvarna SK, Stanley D. The histologic changes of the olecranon fossa membrane in primary osteoarthritis of the elbow. J Shoulder Elbow Surg 2004;13:555-7. https://doi.org/10.1016/s1058274604000928
37. Tamura Y, Sugano N, Sasama T, Sato Y, Tamura S, Yonenobu K, et al. Surface-based registration accuracy of CT-based image-guided spine surgery. Eur Spine J 2005;14:291-7. https://doi.org/10.1007/s00586-004-0797-y
38. Theopold J, Marquass B, von Dercks N, Mutze M, Henkelmann R, Josten C, et al. Arthroscopically guided navigation for repair of acromioclavicular joint dislocations: a safe technique with reduced intraoperative radiation exposure. Patient Saf Surg 2015;9:41. https://doi.org/10.1186/s13037-015-0087-0
39. Tsuge K, Mizuseki T. Débridement arthroplasty for advanced primary osteoarthritis of the elbow. Results of a new technique used for 29 elbows. J Bone Joint Surg Br 1994;76:641-6.
40. Yamamoto M, Murakami Y, Iwatsuki K, Kurimoto S, Hirata H. Feasibility of four-dimensional preoperative simulation for elbow débridement arthroplasty. BMC Musculoskelet Disord 2016;17:144. https://doi.org/10.1186/s12891-016-0996-9